



A numerical study on the formation of upwelling off northeast Taiwan

Chau-Ron Wu,¹ Hung-Fu Lu,¹ and Shenn-Yu Chao²

Received 15 December 2007; revised 19 May 2008; accepted 1 July 2008; published 16 August 2008.

[1] We examined the spatial and temporal variations of upwelling off northeast Taiwan, using a fine-resolution numerical model with realistic bathymetry. The zonally running shelf break in the area deflects the Kuroshio seaward and produces upwelling on its on-shelf edge. The upwelling, in turn, manifests a cold dome or a cyclonic eddy. In depths below 150 m or so, the upwelling and hence the cyclonic eddy exist year-round. Above this depth, the eddy waxes and wanes as the upper portion of the Kuroshio migrates seaward and shoreward, respectively. The eddy event fluctuates in a wide range of timescales. Seasonally, the occurrence heavily favors summer rather than winter, because the mean Kuroshio axis migrates seaward in summer. Intraseasonally, the fluctuation contains two dominant periods centered at 70 days and 30 days. Local wind forcing and channeling by two local canyons do not affect the eddy statistics significantly.

Citation: Wu, C.-R., H.-F. Lu, and S.-Y. Chao (2008), A numerical study on the formation of upwelling off northeast Taiwan, *J. Geophys. Res.*, 113, C08025, doi:10.1029/2007JC004697.

1. Introduction

[2] Seaward deflections of western boundary currents often induce upwelling to fill part of the void. This occurs in a wide range of length scales. On the large-scale side, the reversal of wind stress curl could cause the seaward deflection. The dynamic process may deviate considerably from the present subject of interest. Zooming in to meso-scale, bottom obstacles could also force seaward deflections. On the Pacific side, notable examples include the large meander state of the Kuroshio to the south of Japan, inducing upwelling off Shionomisaki [Shoji, 1972]. On the Atlantic side, a similar process also occurs as the Gulf Stream flows past the so-called Charleston Bump [Xie *et al.*, 2007]. The present paper addresses yet another example of the topography-induced upwelling northeast of Taiwan and its unsteadiness.

[3] A cold dome has often been observed over the edge of the shelf northeast of Taiwan [e.g., Fan, 1980]. Figure 1 shows the topography and oceanography setting. The cold surface water in the area, originated from upwelling, provides a major source of nutrients to support primary production in the East China Sea [Chen, 1996]. The upwelling draws much attention because the exchange between the Kuroshio Water and the East China Sea Shelf Water takes place in that region. The Kuroshio enters the region along the east coast of Taiwan. After leaving Taiwan, the northward flowing Kuroshio bifurcates when it collides with the zonally running shelf [Tang *et al.*, 1999]. The

mainstream turns eastward following the isobaths while a minor branch intrudes onto the shelf over the North Mien-Hua Canyon (NMHC). On the basis of a single cruise of shipboard Acoustic Doppler Current Profiler (Sb-ADCP) in the summer of 1994, Tang *et al.* [1999] demonstrated that the Kuroshio on-shelf intrusion also induces a cyclonic eddy centered over the Mien-Hua Canyon (MHC) about 100 km in diameter.

[4] Historical geomagnetic electrokinetograph measurements concluded that the upper Kuroshio migrates seasonally off northeast Taiwan [Sun, 1987], moving shoreward in fall-winter and seaward in spring-summer. A numerical model with idealized topography and wind forcing [Chao, 1991] lends support to the finding. Conceivably, the seasonal movement of the Kuroshio in upper depths also affects the cyclonic eddy; this is the finding of Tang *et al.* [2000] using three Sb-ADCP observations collected between 1995 and 1997. In summer, the Kuroshio in upper depths generally shifts offshore and the cyclonic eddy is found over the shelf edge northeast of Taiwan. In March of 1997, the upper portion of the Kuroshio shifted shoreward; the cyclonic eddy and the cold dome in upper depths were conspicuously missing. In November of 1991, however, a surface drifter was trapped by the cyclonic eddy northeast of Taiwan, suggesting that the eddy could extend to the surface in winter as well [Tseng and Shen, 2003].

[5] Observations, though revealing, are gappy in time and space. Important issues remain, such as temporal variability and vertical distribution. For example, Sb-ADCP observations are lacking in winter because of the treacherous sea conditions. Further, the intraseasonal variations cannot be fully resolved from existing data. Fine-resolution numerical modeling is called for to address the deficiencies. In this work, we simulate the cyclonic eddy northeast of Taiwan using a fine-resolution model with realistic topography and

¹Department of Earth Sciences, National Taiwan Normal University, Taipei, Taiwan.

²Horn Point Laboratory, Center for Environmental Science, University of Maryland, Cambridge, Maryland, USA.

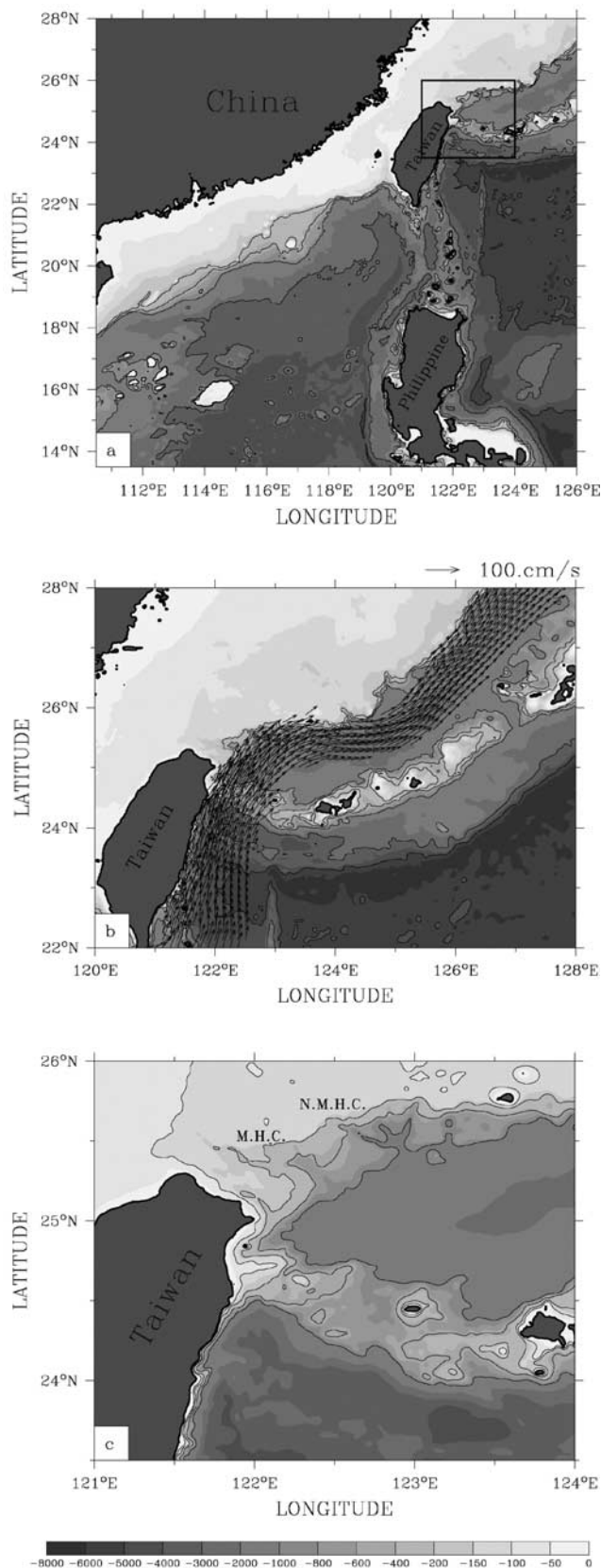


Figure 1. (a) Domain of the SAT model with realistic bathymetry. (b) EAMS-modeled Kuroshio velocity field (vectors); only velocities larger than 40 cm s^{-1} are presented. (c) Bathymetry of the study area. Contours are at 100, 200, 500, 1000, and 5000 m.

forcing. This allows us to examine its temporal and horizontal scales, seasonal and intraseasonal variations, vertical structure and interaction with the Kuroshio.

2. Numerical Model

[6] The Seas Around Taiwan (SAT) model is derived from the sigma-coordinate Princeton Ocean Model (POM) [Blumberg and Mellor, 1987]. The three-dimensional, free surface model solves the primitive equations for momentum, salt and heat. It includes a 2.5-level turbulence closure submodel developed by Mellor and Yamada [1982], and the Smagorinsky [1963] formulation for horizontal mixing. Figure 1a shows the SAT model domain, from 110.5°E to 126°E and from 13.5°N to 28°N , with realistic bathymetry. The horizontal grid size is $1/20^\circ$, and there are 26 sigma levels in the vertical. On open boundaries, the SAT model derives its boundary condition from a larger-scale East Asian Marginal Seas (EAMS) model. The EAMS model is also based on the POM, and has a horizontal resolution of $1/8^\circ$ and 26 sigma levels. The EAMS model domain extends from 99°E to 140°E in longitude, and from 0°N to 42°N in latitude. A detailed description of the EAMS model has been given by Wu and Hsin [2005]. The EAMS model has been validated with observed volume transport of Kuroshio east of Taiwan [Hsin et al., 2008], and corroborated with observed velocity data from both bottom-mounted and shipboard ADCPs in the Taiwan Strait [Wu and Hsin, 2005].

[7] The POM uses the mode splitting technique to separate the vertically integrated governing equations (barotropic or external mode) and the equations governing vertical structure (baroclinic or internal mode). Boundary conditions are separately formulated for the barotropic and baroclinic modes, and then adjusted to take into account the different truncation errors for those modes [Blumberg and Mellor, 1987]. The one-way coupling between the SAT and EAMS models is described below. Following Flather [1976], we derive barotropic velocities on open boundaries of the EAMS model from

$$\bar{u}_n = \bar{u}_n^0 + \sqrt{\frac{g}{H}}(\eta - \eta^0), \quad (1)$$

where \bar{u}_n is the vertically averaged velocity normal to open boundaries of the SAT model at time t , and \bar{u}_n^0 is the corresponding velocity estimated from the EAMS model. The model sea surface height (η), derived from the continuity equation, is located half of a grid inside the open boundary of the SAT model domain. The EAMS model sea surface height (η^0) is located on the open boundary of the SAT model. The water depth on the open boundary is H , and g is the gravitational acceleration. Baroclinic velocities on open boundaries of the SAT model are determined using an inflow condition; daily baroclinic velocities from the EAMS model were spatially interpolated and assigned to the open lateral boundary grids of the SAT model. Temperature and salinity on the open boundaries are subject to advection from upstream; in the case of an inflow, daily EAMS profiles of temperature and salinity provide the upstream values.

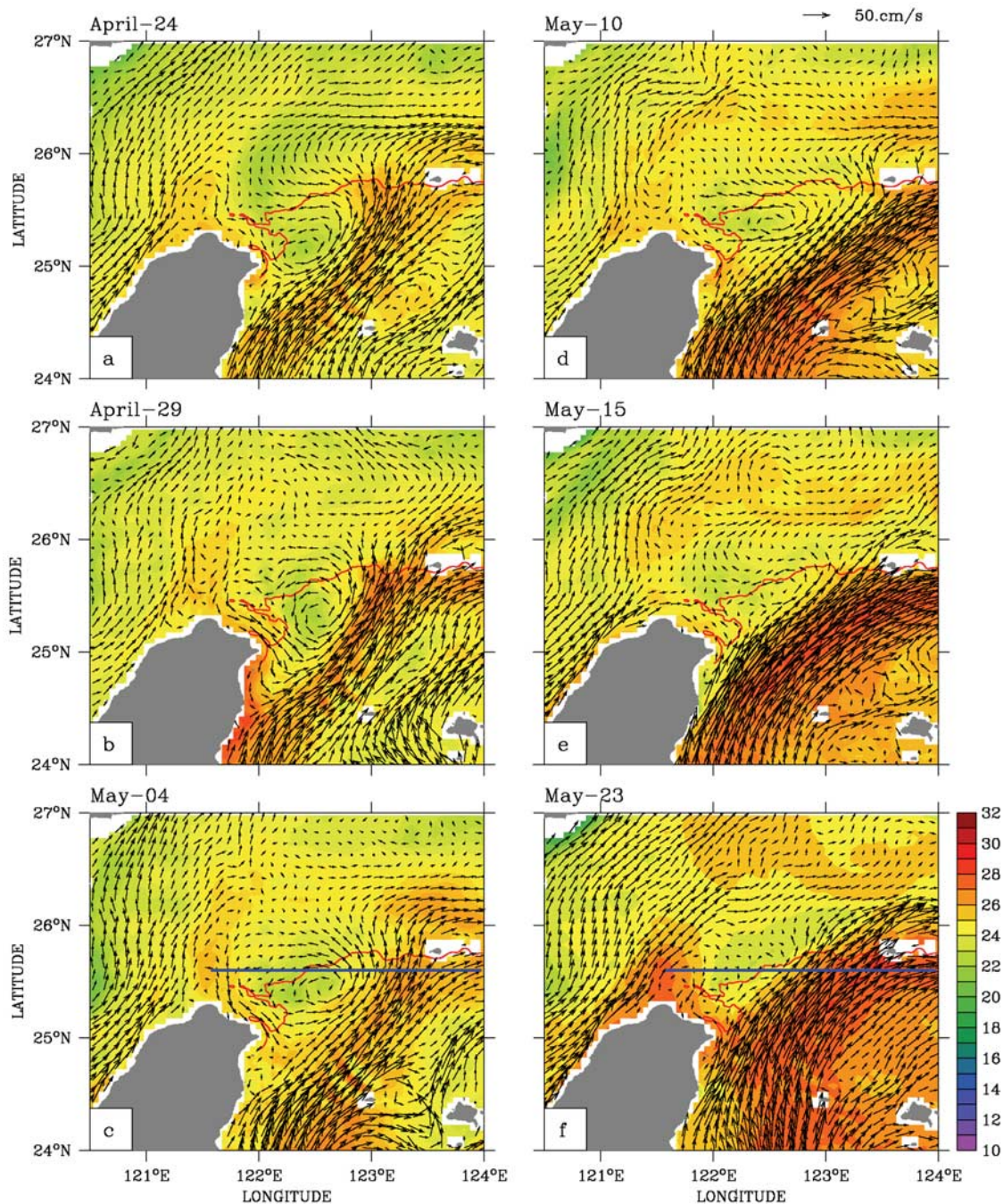


Figure 2. A sequence of model-derived velocity and temperature fields at 20 m on (a) 24 April 1999, (b) 29 April 1999, (c) 4 May 1999, (d) 10 May 1999, (e) 15 May 1999, and (f) 23 May 1999. Red contour indicates 200 m isobath. The zonal blue line indicates the vertical section to be shown in Figure 6.

[8] The SAT model was initialized by temperature and salinity fields of the EAMS model outputs in January 1999, and thereafter subject to climatological forcing for 1 year. After the spin-up period, the SAT model was forced with NASA Quick Scatterometer (QSCAT)/NCEP wind data sets. The blended QSCAT/NCEP wind stress data set is one of the most up-to-date high-resolution data of ocean surface winds at the present time. We adopted 6 hourly maps of 10 m winds at a resolution of $0.5^\circ \times 0.5^\circ$. These fields are derived from a space and time blend of QSCAT-DIRTH satellite scatterometer observations and NCEP

analyses [Milliff *et al.*, 1999]. The SAT model was subject to 6 hourly wind stresses at the sea surface and open ocean boundary forcing (as described above) provided by the EAMS model. The simulation period spans from 1999 to 2003.

3. Results

3.1. Life Cycle of a Cyclonic Eddy

[9] Figure 2 shows snapshots of model-derived velocity and temperature fields at 20 m depth. From 24 April to

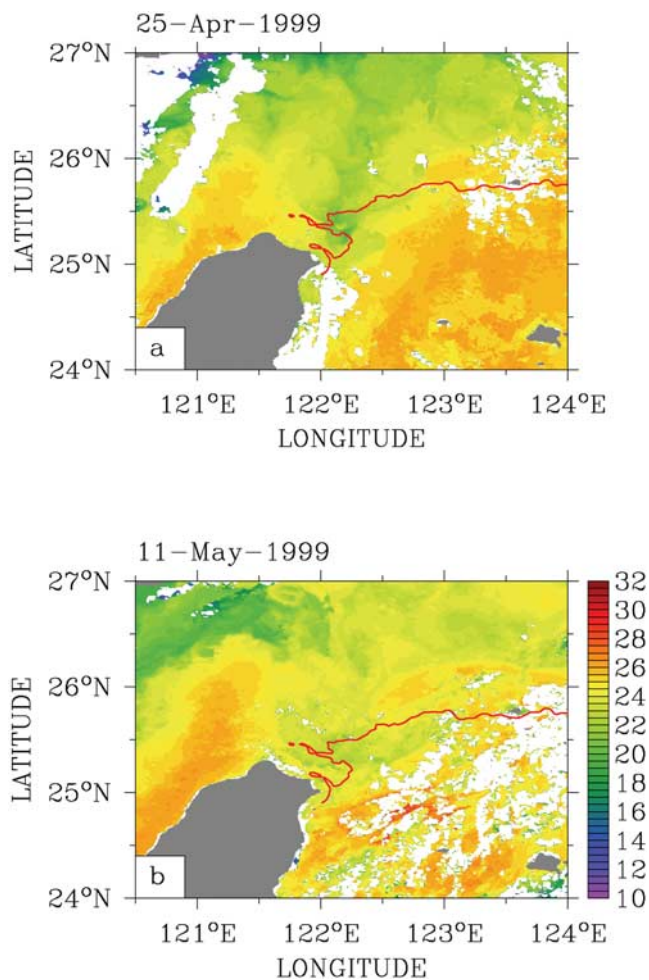


Figure 3. NOAA/advanced very high resolution radiometer images of sea surface temperature on (a) 25 April 1999 and (b) 11 May 1999. Color bar units are $^{\circ}\text{C}$. The red contour indicates the 200 m isobath.

23 May of 1999, the cyclonic eddy varied in size, moved slightly northeastward and gradually vanished after the middle of May. More specifically, on 24 April, the cyclonic eddy about 80 km in diameter was first visible off the northeastern tip of Taiwan. At about 25°N , the Kuroshio with a maximum speed of over 100 cm s^{-1} separated from the continental shelf break. This is the main branch that extended to about 1000 m depth. A minor branch on the inshore side of the Kuroshio intruded onto the continental shelf from NMHC. The minor branch also extended throughout the water column: about 500 m deep over the NMHC and 120 m deep elsewhere over the shelf. As the on-shelf intrusion current entered increasingly shallow water, the potential vorticity constraint would require it to gain clockwise rotation and eventually rejoin the mainstream Kuroshio. A cyclonic eddy, centered at about 25.2°N and 122.4°E , developed to the west of the on-shelf intrusion. Most of the northeastward flowing Taiwan Strait outflow turned northward as it left the Strait. A very small portion of this outflow turned eastward, hugs the northern coast of Taiwan and thereafter feeds the cyclonic eddy (Figure 2a). The cyclonic eddy appeared to expand in time

and its center moved slightly northeastward on 29 April (Figure 2b). On 4 May (Figure 2c), its center moved farther northeastward to about 25.4°N and 122.5°E and, in consequence, the eddy filled a good portion of the region between MHC and NMHC. This cyclonic eddy collocated with the lower-temperature area; its center was about 3°C colder than surrounding waters (Figure 2c). The cyclonic eddy was compressed meridionally on 10 May and the temperature rose slightly in the eddy center (Figure 2d). The eddy shrank and the cyclonic circulation became diffuse on 15 May (Figure 2e). Thereafter the eddy disappeared on 23 May as the Kuroshio migrated shoreward (Figure 2f), completing the life cycle.

[10] The cold dome was also evident in the advanced very high resolution radiometer (AVHRR) image of sea surface temperature on 25 April 1999 (Figure 3a). Similar to the model simulation (Figure 2a), a patch of cold surface water surrounded by warmer water was observed off northeast Taiwan. The sea surface temperature in the cold dome rose on 11 May 1999 (Figure 3b), also consistent with the model simulation (Figure 2d). The evolution of this cold dome shown in the satellite images further confirms the model results.

3.2. Temporal Variability of Surface Upwelling

[11] From model outputs, we have compiled statistics of the cyclonic eddy over the study region from 1 January 1999 to 31 December 2003. Through visual inspection of velocity and temperature fields at 30 m depth, Table 1a shows the onset date of each cyclonic eddy, and Table 1b shows the number of eddies in summer (June, July, and August) and winter (December, January, and February). The number of eddies is maximal in 2000 and minimal in 2001 (Table 1a). Interannual variation aside, there are more eddies in summer than in winter (Table 1b). The lapse between two eddy events also shows seasonal variation: shorter in summer but longer in winter (Table 1a).

[12] Averaging over the 5-year period, Table 1c shows summer, winter and annual mean of the duration and lapse of the eddy events. In summer, each eddy lasted about 12 days and was followed by a 14-day lapse. Thus, upwelling can extend to the surface half of the time in summer. In winter, each eddy lasted only about 6 days and was followed by a 52-day lapse. This seasonal variability is not inconsistent with observations. For example, on the basis of three Sb-ADCP measurements in different seasons

Table 1a. Onset Dates of Eddies From Model Simulation

	Year				
	1999	2000	2001	2002	2003
Onset date of eddies	31 Jan	6 Jan	15 Mar	24 Feb	18 Mar
	9 Feb	3 Apr	4 May	14 Jun	11 Apr
	27 Feb	11 Apr	3 Jun	2 Jul	18 May
	10 Mar	11 May	3 Aug	19 Jul	10 Jun
	10 Apr	28 May	9 Sep	8 Aug	28 Jun
	23 Apr	10 Jun	3 Oct	20 Aug	15 Jul
	9 Jun	15 Jul		17 Oct	15 Aug
	29 Jun	8 Aug		11 Nov	21 Sep
	28 Jul	26 Aug		21 Dec	25 Oct
	28 Aug	23 Sep			21 Dec
	12 Oct	25 Oct			
		28 Nov			

Table 1b. Number of Eddies in Summer and Winter^a

Year	Number of Eddies	
	Summer	Winter
1999	4	3
2000	4	1
2001	2	0
2002	5	1
2003	4	1
Total	19	6

^aSummer includes the months June, July, and August, while winter includes the months December, January, and February.

between 1995 and 1997, *Tang et al.* [2000] found out that the cyclonic eddy existed in summer, but disappeared in March 1997 when the Kuroshio moved shoreward. In terms of the annual mean, eddy events were 10 days long each and sandwiched by a 22-day lapse in between (Table 1c). As the following analysis bears out, this points to an oscillation period of one month.

3.3. Empirical Orthogonal Functions Analysis of Temperature

[13] In terms of temperature, the large seasonal fluctuation often masks intraseasonal fluctuations. To emphasize intraseasonal variability, we remove the annual cycle (the 365-day period) with a harmonic analysis and thereafter apply Empirical Orthogonal Functions (EOF) analysis to the residual temperature field at 20 m depth. The resultant first EOF mode (Figure 4) accounts for 23.3% of the total variance. Two dominant signals stand out in the first mode. There is a large-amplitude oscillation centered at 25.6°N, 122.5°E off northeast Taiwan; another maximum band over the Kuroshio region extends essentially from southwest to northeast (Figure 4a). These two dominant oscillations are in phase. In other words, the cold eddy tends to vanish if the Kuroshio moves shoreward, or appear when the Kuroshio moves seaward. Figure 4b shows temporal variation of the first mode with negative values representing possible appearance of the cold eddy. Intraseasonal variations of this eddy are abundant.

[14] Figure 5 shows the variance-preserving spectrum of the first mode. Two peaks centered at 70 days and 30 days are significant. The 30-day period agrees with the estimated period on the basis of visual inspection (Table 1c). As we will see in section 4, both periods correlate with variations of the Kuroshio.

3.4. Vertical Structure of the Cyclonic Eddy

[15] Vertical flow patterns with and without the eddy differ markedly. On 4 May 1999, the cold eddy was centered at about 25.4°N and 122.5°E (Figure 2c). Figures 6a and 6b show the corresponding vertical sections

Table 1c. Duration of, and Lapse Between, Eddy Events Averaged Over the 5-Year Period^a

	Duration (days)	Time Interval (days)
Summer	12	14
Winter	6	52
Annual mean	10	22

^aSummer includes the months June, July, and August, while winter includes the months December, January, and February.

of eastward (U) and northward (V) velocities, respectively, along 25.6°N, and Figure 6c shows the corresponding temperature section. At this time, the Kuroshio mainstream was located at about 123.75°E off the shelf. It had a subsurface core of eastward velocity (U) at 280 m depth ranging up to 60 cm s⁻¹. Between the shelf and the Kuroshio, the current was westward and spanned nearly the entire water column. Relative to eastward velocity, the meridional velocity was much weaker. A near-surface core of northward current ranging up to 40 cm s⁻¹ existed near the shoreward edge of the eastward flowing Kuroshio mainstream; this is the bifurcated branch of on-shelf Kuroshio intrusion. However, most of the subsurface Kuroshio current turned eastward when colliding with the zonally running shelf. Off the shelf, the current below 150 m depth was southwestward between 122.5 and 122.9°E (near the head of NMHC). This was the upstream of the cyclonic circulation that carried the subsurface Kuroshio water onto the shelf northeast of Taiwan [*Tang et al.*, 1999]. Over the shelf, currents were generally two layered, the surface southward flow being undercut by a northward flow. Overall, the vertical structure was corroborated by observed velocity data when the eddy existed (left panels of Figure 6 in the paper by *Tang et al.* [2000]). Specifically, on the basis

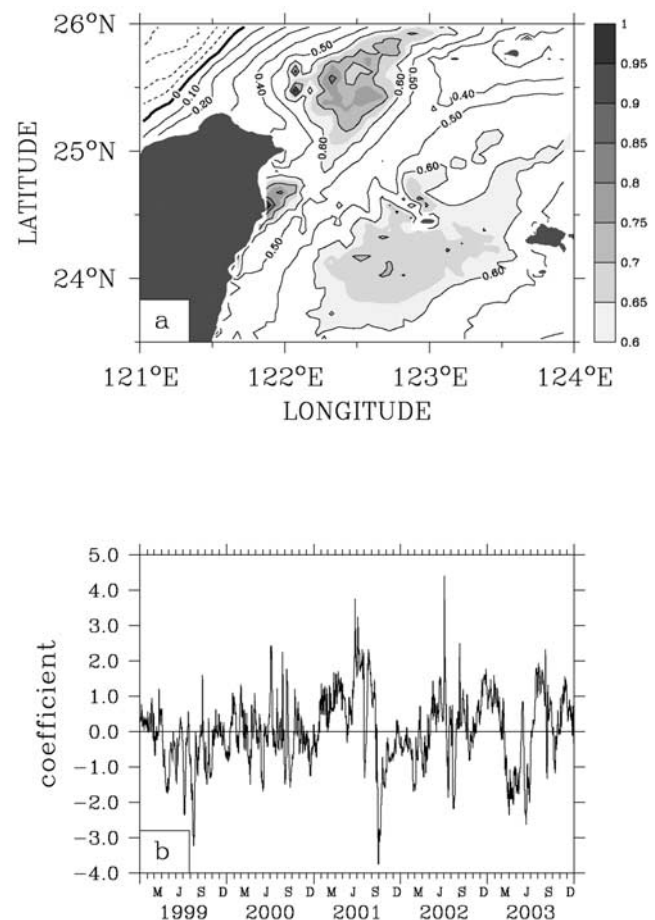


Figure 4. (a) Spatial pattern of the first EOF mode for residual temperature at 20 m depth. Contour intervals are 0.1; light shading indicates contours larger than 0.6. (b) Corresponding temporal variations.

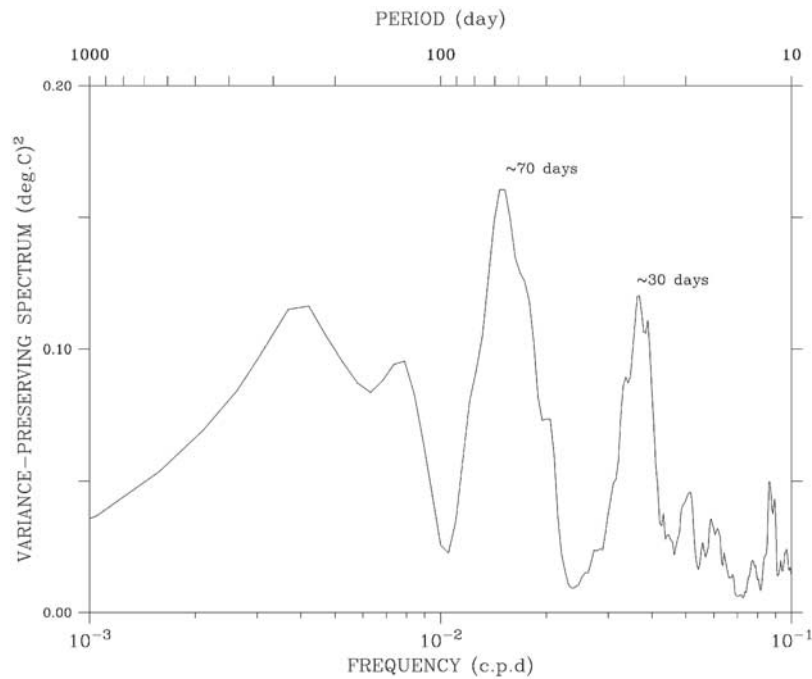


Figure 5. The variance-preserving spectrum for the first EOF mode in Figure 4b.

of composite Sb-ADCP velocity data collected between 1991 and 1997, vertical-zonal section along 25.625°N in the paper by *Tang et al.* [2000] clearly showed a submerged core of eastward moving Kuroshio centered at 250 m depth in summer when the conditions favored the formation of the cyclonic eddy and the cold dome. At this time, the temperature section (Figure 6c) showed elevated isotherms centered over the shelf break.

[16] The eddy vanished in upper depths on 23 May 1999 (Figure 2f). Figures 6d and 6e shows corresponding U and V velocity profiles along 25.6°N ; Figure 6c shows the corresponding temperature section. In terms of eastward current, the Kuroshio expanded shoreward, its core speed increased to more than 90 cm s^{-1} and its core depth rose to around 75 m depth. The southward currents northeast of Taiwan weakened or even disappeared in the upper 100 m or so. The modeled vertical structure is also similar to that derived from Sb-ADCP data when the eddy did not exist (right panels of Figure 6 in the paper by *Tang et al.* [2000]). Specifically, their figure also showed the strengthening and rising of the submerged Kuroshio core. Furthermore, the separation of the northward and eastward current velocity cores indicated the Kuroshio bifurcation. At this time, warmer waters in upper 30 m returned to the shelf to cap the cold dome (Figure 6f).

[17] Although the comparisons between the modeled and the Sb-ADCP velocities were not contemporaneous, they nevertheless point out two distinct mesoscale patterns. When the cold eddy existed, both observation and the present model suggested one pattern with a distinct vertical structure. When the eddy disappeared, both suggested another pattern with a different vertical structure. Prior to this study, the collective wisdom often associated the two distinct patterns with seasons: the eddy state with an offshore Kuroshio axis was identified as summer-like and the noneddy state with an encroaching Kuroshio axis was

identified as winter-like. The seasonality generalization needs to change in light of the present study. Transition between the two states should occur in timescales that transcend seasonality. The alleged summer-like state could occur in winter and the winter-like state could occur in summer. However, the frequency of occurrence favors the summer-like state in summer and winter-like state in winter. The identification of summer and winter states is due more to seasonality in number of occurrences and event duration than to either state being confined to a particular season.

3.5. Upwelling Mechanism

[18] In the northern hemisphere, sea level slopes across entire western boundary currents, with increasing sea level from inshore edge to offshore edge. Seaward migration of the current often creates an area of negative sea level anomaly on its inshore edge. The anomaly, in turn, invites upwelling and development of the cyclonic eddy. A classical analogy in the atmosphere is how a mild tropical depression induces a cyclone and accelerates updraft of moist air from the marine boundary layer [*Charney and Eliassen*, 1964]. In the present setting, blocking of the Kuroshio by the zonally running shelf causes the seaward deflection and should be ultimately responsible for the upwelling. One can easily illustrate the negative pressure anomaly by subtracting a non-eddy-state sea level from an eddy-state sea level. Using Figure 2c as a typical eddy state and Figure 2f as the following noneddy state, the subtraction leads to a pronounced negative sea level anomaly off northeast Taiwan (Figure 7). The dynamic process investigated herein should not be unique. In the South Atlantic Bight, for example, the seaward deflection of the Gulf Stream by the Charleston Bump also induces a cyclonic eddy in the lee [*Xie et al.*, 2007]. Coastal Zone Color Scanner images often showed elevated Chlorophyll concen-

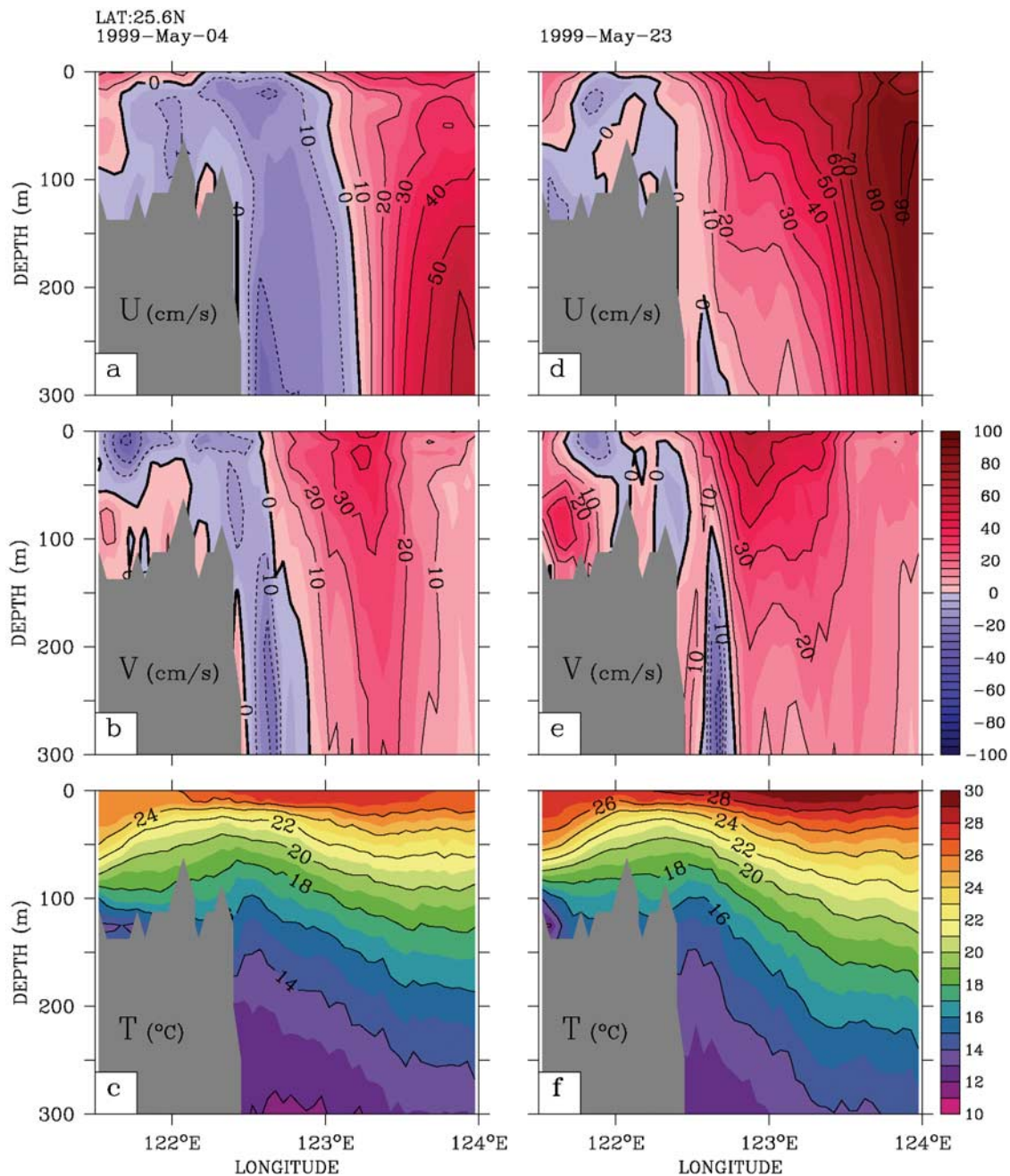


Figure 6. Vertical sections of the cyclonic eddy and Kuroshio along 25.6°N : (a) eastward velocity, (b) northward velocity, and (c) temperature on 4 May 1999. This is the time the eddy existed and centered at about 25.4°N and 122.5°E . After the eddy vanished on 23 May 1999, corresponding vertical sections are shown for (d) eastward velocity, (e) northward velocity, and (f) temperature. Solid velocity contours indicate eastward flow for U and northward flow for V . Dashed contours indicate opposite currents.

tration in the same region (C. R. McClain, private communication, 1987), indicative of upwelling.

[19] Figures 8a and 8b show 5-year averages of the model velocity and temperature fields at 30m in summer (June, July, and August) and winter (December, January, and February), respectively. Several features similar to observations stand out. *Liang et al.* [2003] provided the most detailed description to date for the mean state of the Kuroshio in the upper ocean east of Taiwan on the basis of 10 years' (1991–2000) Sb-ADCP data. Consistent with

their finding, the modeled Kuroshio flows northward along the east coast of Taiwan, turning northeastward near 24.5°N and following the continental slope thereafter. A notable difference between Figures 8a and 8b is the conspicuous presence of the cold cyclonic eddy in summer only. Past observations, though sparse, capture these mean states.

[20] Corresponding features at 200 m depth (Figures 8c and 8d) reveal more. The cyclonic eddy shows up in summer as expected (Figure 8c). It also shows up in winter at this depth (Figure 8d). In fact, the cyclonic eddy at depths

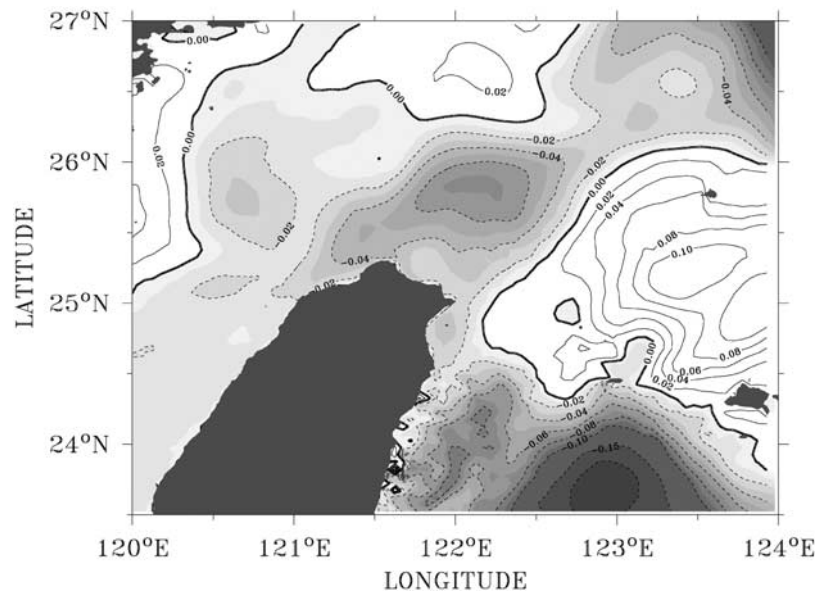


Figure 7. The sea level difference between eddy state on 4 May 1999 and noneddy state on 23 May 1999. Negative (positive) values correspond to low (high) sea level for the eddy state. Contours are from -0.1 m to 0.1 m at intervals of 0.02 m.

is found in all months of the year (figures not shown), suggesting year-round upwelling. However, occasional capping by the warm Kuroshio water would limit the upwelling to deeper depths. A bottom-mounted ADCP deployed nearby [Tang and Yang, 1993] supports the winter existence of the cyclonic eddy at depths. The eddy would extend to the surface when the Kuroshio moves seaward. Conversely, the Kuroshio encroachment, whether seasonal or intraseasonal, would mask the surface signature of this eddy.

[21] Figure 9 shows the temporal variability of the kinetic energy at 20 m along 25.5°N from 5 years of model simulation. Kinetic energy is defined as $Ke = 1/2 (u^2 + v^2)$. Figure 9a shows a turquoise band containing relatively large kinetic energy zonally oscillating between east and west of 123°E . To its west is a zone of much weaker kinetic energy. The turquoise band, roughly representing the mainstream of the Kuroshio, contains seasonal variations. Large kinetic energy extended as far west as 122.6°E near wintertime, but retreated to east of 123.2°E during summertime. The seasonal migration was noted earlier [Chao, 1991; Tang et al., 2000]. The Kuroshio path at this upper depth also contains intraseasonal fluctuations. For example, Figure 9b is a close-up view from 15 April to 15 August 1999. The kinetic energy was not strong until 10 May when it exceeded $0.5 \text{ m}^2 \text{ s}^{-2}$. It weakened again in early June and reached another maximum after the middle of June. The peak persisted only for a week and weakened thereafter from late June to middle July. In other words, the Kuroshio migrated even within a single month, affecting the cyclonic eddy in upper depths. To illustrate this, four eddy events are delineated by rectangles in Figure 9b, lasting 7–18 days each. After each eddy event, the kinetic energy increased markedly, indicating the on-shelf return of the Kuroshio.

[22] We have also investigated the wind and topographic effects on upwelling. After turning off the wind forcing, features off northeast Taiwan are similar to Figure 2. Apparently, local wind forcing is not responsible for the

upwelling. The collision of the Kuroshio with the zonally running slope must be ultimately responsible. Moreover, experiments without MHC and or NMHC do not markedly impact the formation of upwelling (figures not shown). In other words, NMHC and MHC may provide easy conduits for the on-shelf Kuroshio intrusion and cold eddy formation, but these processes will survive without them.

4. Discussion

[23] Although long-term measurements of the upwelling are unavailable, snapshots indicated that the upwelling in the region contains different timescales. In noting the unexplained absence of counterclockwise circulation in the Sb-ADCP composite flow pattern in summer, Tang et al. [2000] suggested that the upwelling in the region may contain not only seasonal but also intraseasonal variations. Their four snapshots of cruise data also showed that the upwelling center in the same season might vary in strength and location from year to year. The present model simulation supports their suggestion. Further, the model has identified 70-day and 30-day oscillations associated with the eddy event. Intuitively, the variability of the local wind forcing or the Kuroshio migration may be suspects responsible for these oscillations. However, the spectrum of 5-year QSCAT/NCEP wind data does not contain these oscillations, and the development of upwelling does not correlate with the local wind stress or its curl in any significant way (figure not shown). Local wind forcing is therefore not responsible. On the other hand, the model result points to the Kuroshio migration as the cause of these oscillations.

[24] Intraseasonal variability of the Kuroshio east of Taiwan was well documented by Johns et al. [2001] and Zhang et al. [2001]. The variability, in turn, causes intraseasonal fluctuations of upwelling. On the basis of a mooring array deployed along the profiling current meter-1 (PCM-1) line during the World Ocean Circulation Exper-

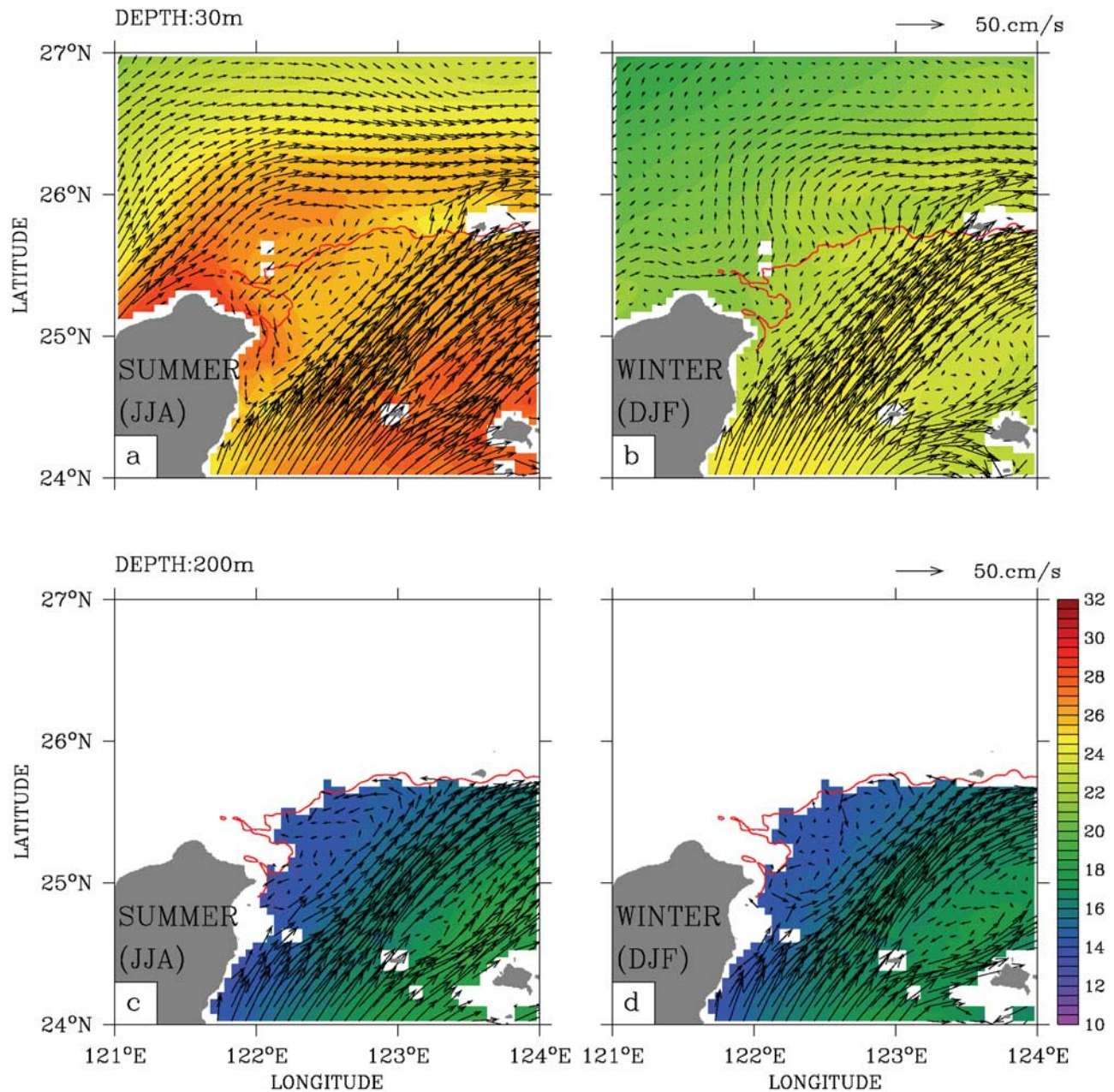


Figure 8. The 5-year average of the model velocity and temperature fields at 30 m in (a) summer (June, July, and August) and (b) winter (December, January, and February). Corresponding features at 200 m depth are shown for (c) summer and (d) winter. Velocities are in cm s^{-1} , and temperatures are in $^{\circ}\text{C}$. The red contour indicates 200 m isobath.

iment over a 20-month period (between September 1994 and May 1996), the estimated Kuroshio transport contained a dominant period of about 3–4 months [Johns *et al.*, 2001]. According to the EOF analyses of the PCM-1 array data, Zhang *et al.* [2001] further pointed out that the two leading modes (transport mode and meandering mode) had a significant energy peak at 70–200 days. Their transport mode had a secondary peak near 30 days. Furthermore, satellite altimeter data and drifter studies concluded that the Kuroshio fluctuations at periods about 2–4 months are caused by the westward propagation of mesoscale eddies from the interior of the Pacific Ocean [e.g., Yang *et al.*,

1999; Yang and Liu, 2003; Hwang *et al.*, 2004]. Yang *et al.* [1999] further suggested that the Kuroshio transport fluctuated with eddy impingements: a cyclonic eddy impinging on the Kuroshio would reduce its transport, and an anticyclonic eddy impinging on the Kuroshio would increase its transport. Advancement aside, the cause of these eddy impingements centered at 70-day period is still unresolved, noting that simple theoretical ideas do not work well in this complex environment. For example, the propagation of baroclinic Rossby waves from the eastern boundary of the Pacific to this area takes much longer than 70 days [Cane, 1983]. Even more elusively, all previous investigations

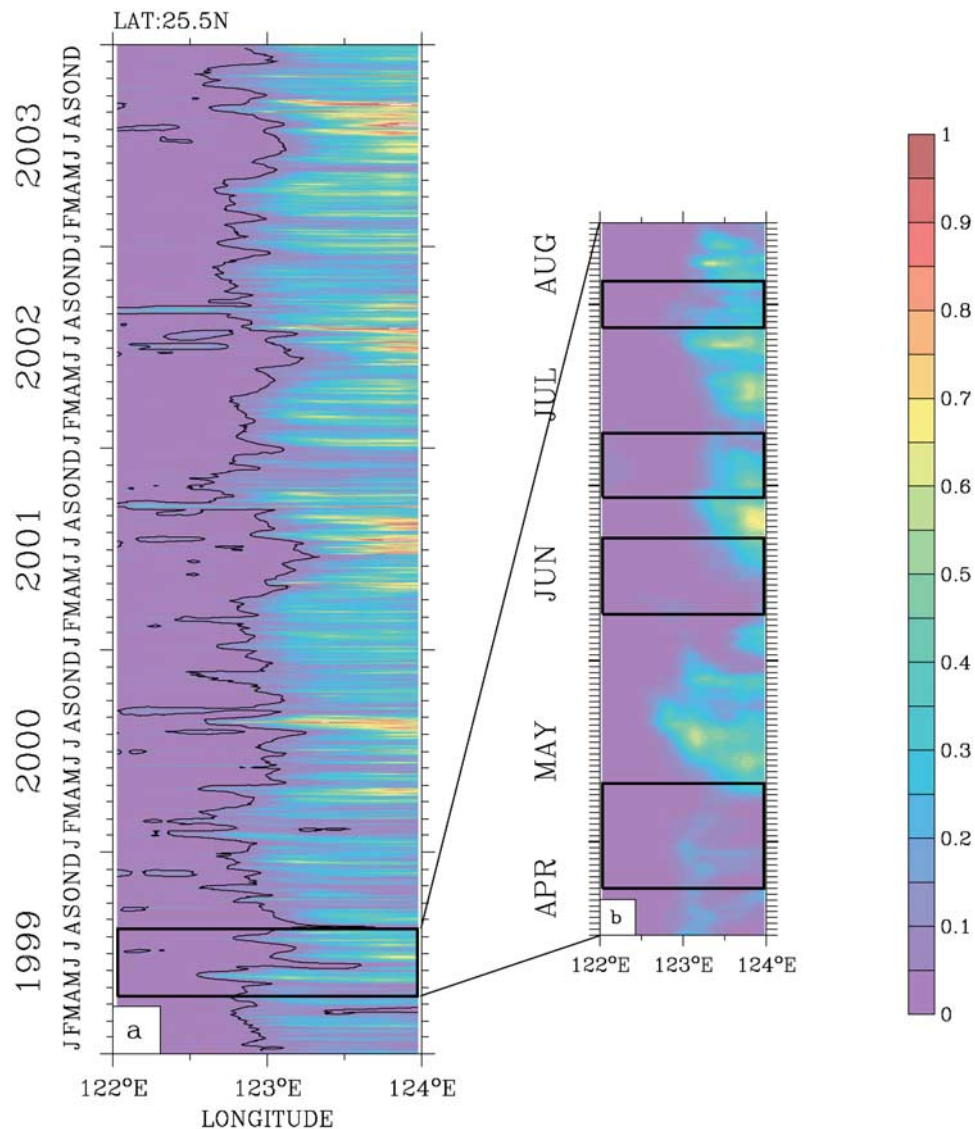


Figure 9. (a) Temporal variability of the kinetic energy at 20 m along 25.5°N over 5 years of model simulation. (b) The 4-month episode from 15 April to 15 August 1999. Color bar units are $\text{m}^2 \text{s}^{-2}$.

failed to identify the mechanism leading to the 30-day oscillation. It has also eluded our extensive scrutiny, still unresolved.

[25] To illustrate the depth scale of the Kuroshio migration, Figure 10 shows time series of northward component (V) along 25.25°N over the 5-year period at 30, 100, 150, 200, and 250 m depths. In general, the migration decreased with depth and was mostly confined in the upper 150 m. This explains why event-like Kuroshio encroachments failed to mask the year-round upwelling at 200 m depth (Figure 8). *Liu et al.* [1992] reached a similar conclusion on the basis of chemical hydrography. According to them, the upwelling over the shelf break northeast of Taiwan occurred year-round, and it occasionally reached the sea surface as a pool of cold and nutrient-rich surface water.

[26] To quantify further, we have calculated the vertical gradient of the standard deviation of temperature for the 5-year period, and identified the depth where its vertical slope is the steepest. Mathematically, this is the depth where

the second vertical derivative is maximal for the standard deviation of temperature (Figure 11). Away from the area of interest, this depth is about 75 m, the mixed layer depth. In the area of interest, this depth is about 150 m, the depth scale for the Kuroshio migration. According to the recent hydrographic sections compiled by the National Center for Ocean Research (data are available at <http://140.112.65.17/odbs/Physics/ctd/ctdprof.php>), the Kuroshio axis in this region is defined by 20°C isotherm at 150 m, the depth of maximum salinity (34.8). This is consistent with our finding.

5. Concluding Remarks

[27] We have examined the spatial and temporal variations of upwelling off northeast Taiwan, using a three-dimensional numerical model. Upwelling manifests a cyclonic eddy that originates near the southern East China Shelf. The temperature near the eddy center is about 3°C colder than surrounding waters. The AVHRR images of sea

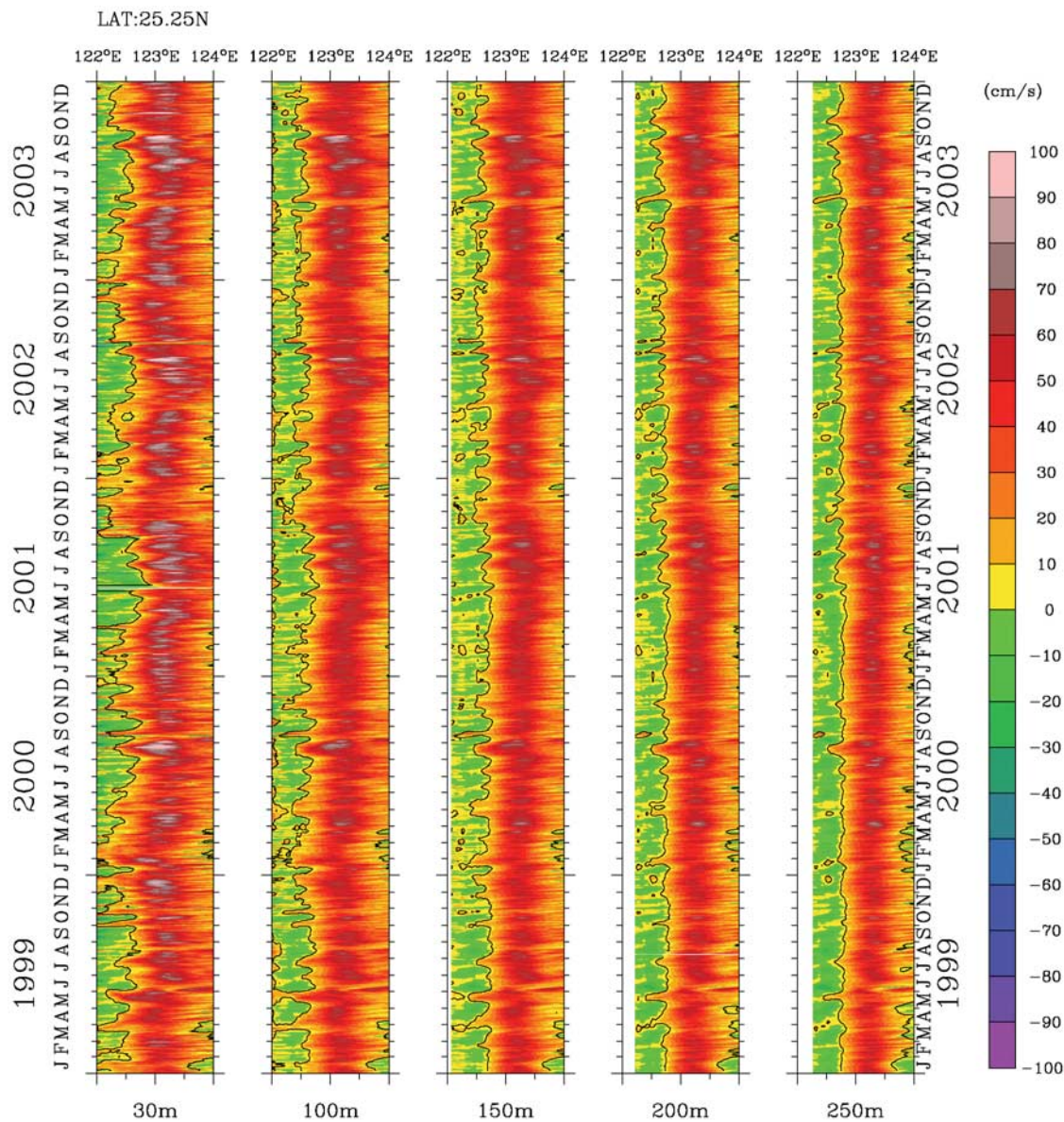


Figure 10. Cross section of northward velocity component along 25.25°N over the 5-year period at depths of 30 m, 100 m, 150 m, 200 m, and 250 m. Color bar units are cm s^{-1} .

surface temperature compare favorably with the model results. Modeled velocity profiles along 25.6°N also agree with composite Sb-ADCP velocity data. Below 150 m or so, the cold eddy exists all year-round. In upper depths, the Kuroshio migration regulates the eddy event. An eastward (seaward) migration of the Kuroshio favors the formation of a cyclonic eddy and a cold dome in upper depths. On the other hand, the cyclonic eddy in upper depths disappears when the Kuroshio moved westward (shoreward). The cold eddy in upper depths appears more frequently in summer than in winter. In general, each eddy in upper depths also survives longer in summer than in winter, resulting in shorter lapses between eddy events in summer. Collectively, the foregoing results provide a logical explanation that bridges gaps among sparse observations in the past.

[28] After removing the annual cycle, the leading EOF mode accounts for 23.3% of the total variance. It contains

two areas of large-amplitude oscillations: one off northeast Taiwan and the other over the Kuroshio region. Both oscillations are in phase, indicating that the cold eddy waxes and wanes as the Kuroshio moves seaward and shoreward, respectively. Temporal variation of the first mode shows 70-day and 30-day oscillations, the dominant timescales of the Kuroshio migration. The migration is active only in the upper 150 m or so; this explains the eddy's vulnerability above this depth and lack thereof below.

[29] The average upwelling rate can also be estimated from the model. Over the upwelling region (from 122.25°E to 122.75°E in longitude, and from 25.1°N to 25.6°N in latitude), the average upwelling rate over the 5-year period is 5.5 m d^{-1} in the upper 60 m. For the upwelling domain of 2800 km^2 , the total upwelling transport is about 0.16 Sv ($1 \text{ Sv} = 10^6 \text{ m}^3 \text{ s}^{-1}$). Previous observation-based estimates are comparable; the corresponding upwelling rate and

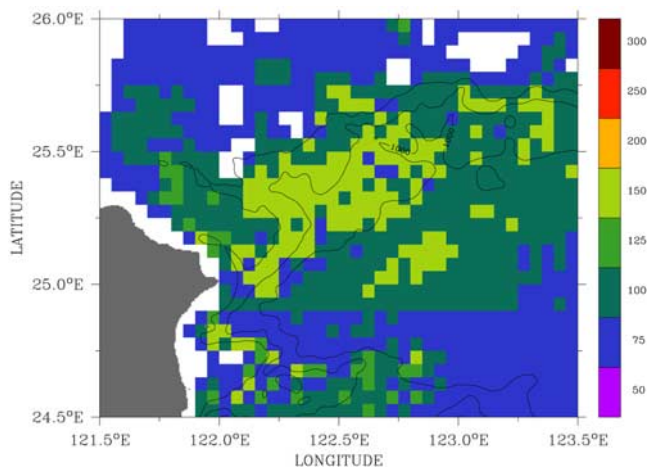


Figure 11. Depths of active temperature gradient layer. The second vertical derivative for the standard deviation of temperature is maximal on this surface. Color bar units are m.

upwelling transport are 5.4 m d^{-1} and 0.2 Sv , respectively [Liu *et al.*, 1992].

[30] **Acknowledgments.** The authors would like to thank the two anonymous reviewers for their careful review of the manuscript and detailed suggestions to improve the manuscript. Author C.R.W. was supported by the National Science Council, Taiwan, ROC, under grant NSC 95-2611-M-003-001-MY3. Author S.Y.C. was supported by U. S. Office of Naval Research, Code 322 PO under contract N00014-05-1-0279. This is UMCES contribution 4202.

References

- Blumberg, A. F., and G. L. Mellor (1987), A description of a three-dimensional coastal ocean circulation model, in *Coastal and Estuarine Sciences*, vol. 4, *Three-Dimensional Coastal Models*, edited by N. S. Heaps, pp. 1–16, AGU, Washington, D. C.
- Cane, M. A. (1983), Oceanographic events during El Niño, *Science*, *222*, 1189–1195, doi:10.1126/science.222.4629.1189.
- Chao, S. Y. (1991), Circulation of the East China Sea, a numerical study, *J. Oceanogr.*, *42*, 273–295.
- Charney, J. G., and A. Eliassen (1964), On the growth of the hurricane depression, *J. Atmos. Sci.*, *21*, 68–75, doi:10.1175/1520-0469(1964)021<0068:OTGOTH>2.0.CO;2.
- Chen, C. T. A. (1996), The Kuroshio intermediate water is the major source of nutrients on the East China Sea continental shelf, *Oceanol. Acta*, *5*, 523–527.
- Fan, K. L. (1980), On the upwelling off northeastern shore of Taiwan, *Acta Oceanogr. Taiwan.*, *11*, 105–117.
- Flather, R. A. (1976), A tidal model of the north-west European continental shelf, *Mem. Soc. R. Sci. Liege*, *6*, 141–164.
- Hsin, Y.-C., C.-R. Wu, and P.-T. Shaw (2008), Spatial and temporal variations of the Kuroshio east of Taiwan, 1982–2005: A number study, *J. Geophys. Res.*, *113*, C04002, doi:10.1029/2007JC004485.
- Hwang, C., C.-R. Wu, and R. Kao (2004), TOPEX/Poseidon observations of mesoscale eddies over the subtropical countercurrent: Kinematic characteristics of an anticyclonic eddy and a cyclonic eddy, *J. Geophys. Res.*, *109*, C08013, doi:10.1029/2003JC002026.
- Johns, W. E., T. N. Lee, D. Zhang, R. Zantopp, C.-T. Liu, and Y. Yang (2001), The Kuroshio east of Taiwan: Moored transport observations from WOCE PCM-1 array, *J. Phys. Oceanogr.*, *31*, 1031–1053, doi:10.1175/1520-0485(2001)031<1031:TKEOTM>2.0.CO;2.
- Liang, W.-D., T. Y. Tang, Y. J. Yang, M. T. Ko, and W.-S. Chuang (2003), Upper-ocean currents around Taiwan, *Deep Sea Res., Part II*, *50*, 1085–1105, doi:10.1016/S0967-0645(03)00011-0.
- Liu, K.-K., G.-C. Gong, S. Lin, C.-Y. Yang, C.-L. Wei, S.-C. Pai, and C.-K. Wu (1992), The year-round upwelling at the shelf break near the northern tip of Taiwan as evidenced by chemical hydrography, *Terr. Atmos. Oceanic Sci.*, *3*, 243–276.
- Mellor, G. L., and T. Yamada (1982), Development of a turbulence closure model for geophysical fluid problems, *Rev. Geophys.*, *20*, 851–875, doi:10.1029/RG020i004p00851.
- Milliff, R. F., W. G. Large, J. Morzel, G. Danabasoglu, and T. M. Chin (1999), Ocean general circulation model sensitivity to forcing from scatterometer winds, *J. Geophys. Res.*, *104*, 11,337–11,358, doi:10.1029/1998JC900045.
- Shoji, D. (1972), Time variation of the Kuroshio south of Japan, in *Kuroshio, Physical Aspects of the Japan Current*, edited by H. Stommel and K. Yoshida, pp. 217–234, Univ. of Wash. Press, Seattle, Wash.
- Smagorinsky, J. (1963), General circulation experiments with the primitive equations. I. The basic experiments, *Mon. Weather Rev.*, *91*, 99–164, doi:10.1175/1520-0493(1963)091<0099:GCEWTP>2.3.CO;2.
- Sun, X. (1987), Analysis of the surface path of the Kuroshio in the East China Sea, in *Essays on Investigation of Kuroshio*, edited by X. Sun, pp. 1–14, China Ocean Press, Beijing.
- Tang, T. Y., and Y. J. Yang (1993), Low frequency current variability on the shelf break northeast of Taiwan, *J. Oceanogr.*, *49*, 193–210, doi:10.1007/BF02237288.
- Tang, T. Y., Y. Hsueh, Y. J. Yang, and J. C. Ma (1999), Continental slope flow northeast of Taiwan, *J. Phys. Oceanogr.*, *29*, 1353–1362, doi:10.1175/1520-0485(1999)029<1353:CSFNOT>2.0.CO;2.
- Tang, T. Y., J. H. Tai, and Y. J. Yang (2000), The flow pattern north of Taiwan and the migration of the Kuroshio, *Cont. Shelf Res.*, *20*, 349–371, doi:10.1016/S0278-4343(99)00076-X.
- Tseng, R.-S., and Y.-T. Shen (2003), Lagrangian observations of surface flow patterns in the vicinity of Taiwan, *Deep Sea Res., Part II*, *50*, 1107–1115, doi:10.1016/S0967-0645(03)00012-2.
- Wu, C.-R., and Y.-C. Hsin (2005), Volume transport through the Taiwan Strait: A numerical study, *Terr. Atmos. Oceanic Sci.*, *16*, 377–391.
- Xie, L., X. Liu, and L. J. Pietrafesa (2007), Effect of bathymetry curvature on Gulf Stream instability in the vicinity of the Charleston Bump, *J. Phys. Oceanogr.*, *37*, 452–475, doi:10.1175/JPO2995.1.
- Yang, Y., and C.-T. Liu (2003), Uncertainty reduction of estimated geostrophic volume transports with altimeter observations east of Taiwan, *J. Oceanogr.*, *59*, 251–257, doi:10.1023/A:1025503624314.
- Yang, Y., C.-T. Liu, J.-H. Hu, and M. Koga (1999), Taiwan Current (Kuroshio) and impinging eddies, *J. Oceanogr.*, *55*, 609–617, doi:10.1023/A:1007892819134.
- Zhang, D., T. N. Lee, W. E. Johns, C.-T. Liu, and R. Zantopp (2001), The Kuroshio east of Taiwan: Modes of variability and relationship to interior ocean mesoscale eddies, *J. Phys. Oceanogr.*, *31*, 1054–1074, doi:10.1175/1520-0485(2001)031<1054:TKEOTM>2.0.CO;2.
- S.-Y. Chao, Horn Point Laboratory, Center for Environmental Science, University of Maryland, Cambridge, MD 21613-0775, USA.
- H.-F. Lu and C.-R. Wu, Department of Earth Sciences, National Taiwan Normal University, Number 88, Section 4 Ting-Chou Road, Taipei 11677, Taiwan. (cwu@ntnu.edu.tw)